CHEMISTRY OF MATERIALS
Article

Chem. Mater. **2010,** *22,* 4007–4018 4007
DOI:10.1021/cm100592x

Structural Characteristics, Electronic Structure, and Thermoelectric Property of New Sb-Based Type-I Clathrates from Density Functional Theory Calculations

Long-Hua Li,[†,‡] Ling Chen,*[,†] Jun-Qian Li[§] and Li-Ming Wu*[,†]

[†]*State Key Laboratory of Structural Chemistry, Fujian Institute of Research on the Structure of Matter, Chinese Academy of Sciences, Fuzhou, Fujian, 350002, People's Republic of China,* [‡]*Graduate School of Chinese Academy of Sciences, Beijing, 100039, People's Republic of China, and* [§]*Department of Chemistry, Fuzhou University, Fuzhou, Fujian 350002, People's Republic of China*

Received February 25, 2010. Revised Manuscript Received May 18, 2010

A new Sb-based type-I clathrate family involving group 11 or 12 elements has been studied by density functional theory (DFT) calculations. The hypothetical Cu/Ag−Sb- and Zn/Cd−Sb-based compounds are studied in stoichiometry, site preference, and electronic structure. The transport properties of some of the energetically favorable compounds have been evaluated. The Ba 5d states in Sb-based clathrates contribute an important component to the valence bands, and Cd and Zn in Zn/Cd−Sb-based clathrates show different site preference from Ga in Ba−Ga−Ge clathrates. Although most of the Sb-based type-I clathrate compounds are metallic in nature, some of them can undergo a metal-to-semiconductor transition via changing the guest-to-frame atom ratio or introducing Sb vacancy.

Introduction

During the past few years, great efforts have been focused on the inorganic clathrate compounds that have a general formula as $A_xTr_yTt_{46-y-z}\square_z$, where □ is a vacancy, A is an alkali metal (Na, K, Rb, Cs) or alkaline-earth metal (Ca, Sr, Ba), and Tr or Tt represent triel (Tr = B, Al, Ga, In) or tetrel (Tt = Si, Ge, Sn), respectively. Some of them are well-known compounds, such as $Ba_8Ga_{16}Ge_{30}$, $Ba_8Ga_{16}Sn_{30}$, and $Sr_8Ga_{16}Ge_{30}$,[1] and some of them are newly made, for example $(Sr, Eu)_xBa_{8-x}Al_{14}Si_{31}$.[2] These Si- and Ge-based type-I clathrate compounds have been attracting scientific interest because of not only the complex structure that are constructed by two different guest-centered polyhedral cages but also the promising high-temperature thermoelectric properties that may have applications in cooling devices and power generators.

A typical type-I clathrate (cubic space group $Pm\bar{3}n$) has a total of 46 atoms in the unit cell arranged in a 3D framework structure that can be grouped into two types of cages: big tetrakaidecahedron (24-atom) and small dodecahedron (20-atom) (Figure 1a). These frame atoms belong to three crystallographic distinctive sites 6*c*, 16*i*, and 24*k*, in which the 6*c* sites are alone on the 24-atom cage; the 16*i* and 24*k* sites are found on both two cages. The local coordination of each site as shown in Figure 1b is a 4-fold coordinated tetrahedron. Each 24*k*-site is bonded to one 6*c*, two 16*i*, and another 24*k* site; the 6*c*-site is bonded to four 24*k* sites; and the 16*i*-site is bonded to another 16*i* and three 24*k* sites. The site configuration greatly affects both the band structure and the transport property of a heteroelemental clathrate.[30] A random Ga/Ge disorder in $Ba_8Ga_{16}Ge_{30}$ over the frame sites disagrees with the results of the maximum entropy and nuclear magnetic resonance.[3] Ga prefers the 6*c* site to the 16*i* site in $Ba_8Ga_{16}Ge_{30}$.[3−6] The dopant, Cu, Ni, or Zn, in $Ba_8Cu_{6-x}Ge_{40+x}$,[7] $Ba_8Ni_6Ge_{40}$,[8] or $Ba_8Zn_8Ge_{38}$,[9] respectively, prefers the 6*c* site, whereas Tt atom prefers the 16*i* site.

Considering a pnicogen (Pn)-based clathrate, will the site preference on a Pn-based framework be the same as that on the Tt-based framework? This is the first question we will explore in this paper. The atomic site preference is common in other compounds too, such as Gd and Y prefer different metal sites in $Gd_{5-x}Y_xTt_4$ (Tt = Si or Ge) and Si prefers sites within the slab whereas Ge between slabs in $Gd_5(Si_xGe_{1-x})_4$.[10,11] How the atoms are ordered over sites in solids is called a "coloring problem",[12,13] and the moment method is applied to study the relationship

(1) Sales, B. C.; Chakoumakos, B. C.; Jin, R.; Thompson, J. R.; Mandrus, D. *Phys. Rev. B* **2001**, *63*, 245113.
(2) Condron, C. L.; Kauzlarich, S. M. *Inorg. Chem.* **2007**, *46*, 2556–2562.
(3) Nick, P. B.; Dan, B.; Susan, L.; Lone, M.; Galen, D. S.; Horia, M. *J. Chem. Phys.* **2001**, *114*, 10063–10074.
(4) Bentien, A.; Nishibori, E.; Paschen, S.; Iversen, B. B. *Phys. Rev. B* **2005**, *71*, 144107.
(5) Nolas, G. S.; Weakley, T. J. R.; Cohn, J. L.; Sharma, R. *Phys. Rev. B* **2000**, *61*, 3845–3850.
(6) Paschen, S.; Carrillo-Cabrera, W.; Bentien, A.; Tran, V. H.; Baenitz, M.; Grin, Y.; Steglich, F. *Phys. Rev. B* **2001**, *64*, 214404.
(7) Johnsen, S.; Bentien, A.; Madsen, G. K. H.; Iversen, B. B.; Nygren, M. *Chem. Mater.* **2006**, *18*, 4633–4642.
(8) Bentien, A.; Johnsen, S.; Iversen, B. B. *Phys. Rev. B* **2006**, *73*, 094301.
(9) Christensen, M.; Iversen, B. B. *J. Phys.: Condens. Matter* **2008**, *20*, 104244.
(10) Misra, S.; Miller, G. J. *J. Am. Chem. Soc.* **2008**, *130*, 13900–13911.
(11) Misra, S.; Miller, G. J. *J. Solid State Chem.* **2006**, *179*, 2290–2297.
(12) Burdett, J. K. *J. Am. Chem. Soc.* **1980**, *102*, 450–460.
(13) Burdett, J. K.; Lee, S.; McLarnan, T. J. *J. Am. Chem. Soc.* **1985**, *107*, 3083–3089.

Published on Web 06/04/2010

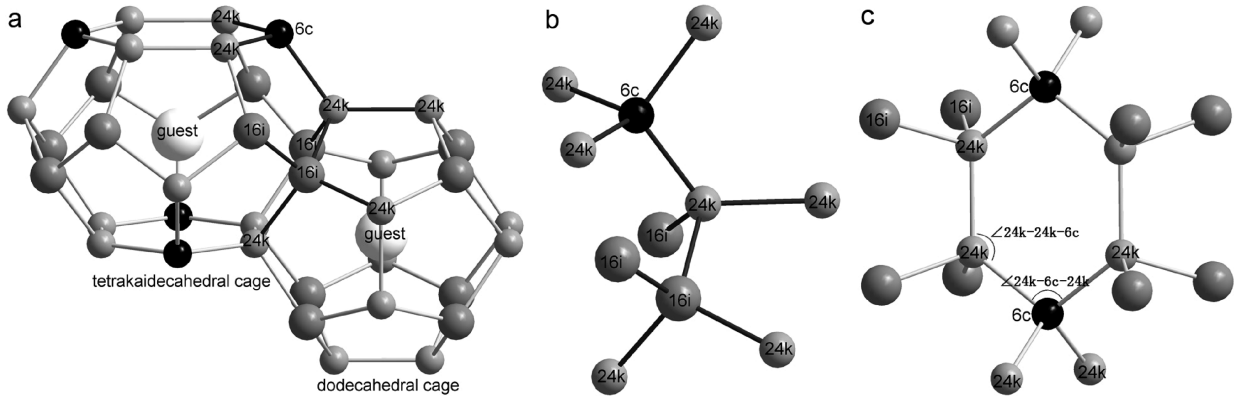

Figure 1. Main structural motifs of a type-I clathrate: (a) geometries of tetrakaidecahedron, dodecahedron, and their connection; (b) local coordination spheres of 6*c*, 16*i*, and 24*k* sites and their geometrical correlations; and (c) the six-membered ring of a tetrakaidecahedron with the crystallographic site and the local coordination environment of each apex marked.

between the structure and the electronic stability in the related compounds.[14−16]

For a better thermoelectric property that is characterized by a high figure of merit ZT ($ZT = S^2\sigma T/\kappa$, T, temperature), a balance among the thermal conductivity (κ), electrical conductivity (σ), and Seebeck coefficient (S) is necessary. Studies show that heavily doped compound or compound with composition slightly shifted away from the "ideal" stoichiometry can exhibit a carrier concentration-related thermoelectric property. For example, as the doping level of $Sr_8Ga_{16}Ge_{30}$ varies from -1.01×10^{19} to -6.03×10^{20} cm^{-3}, the Seebeck coefficient decreases from -313 to -70 μV/K, electrical conductivity increases from 78 to 1250 S/cm, and consequently, the ZT value varies from 0.18 to 0.27.[17] In this case, the doping serves as a chemical modification that does not alter the band structure. On the other hand, few studies show that a minor change of the band structure can also slightly increase the thermoelectric property. Such as in $A_8Ga_{16}Si_xGe_{30-x}$ ($x \leq 15$, A = Ba or Sr), the coupling of the electronic states of Si dopant leads to the slight increases in both the Seebeck coefficient and electrical conductivity.[18,19]

However, up until now, no report has focused on either the band structure or the thermoelectric property of a Pn-based clathrate. As shown above, a moderate band structure-modification on the Tt-based clathrate may have a positive effect on the thermoelectric property. Since the main component of a Pn-based clathrate is different from that of the Tt-based clathrate, their band structures will be different. Therefore, the second question we are interested is as following: what is the unique character of the band structure of the Pn-based clathrates and will the feature provide a positive effect on the thermoelectric property?

In this paper, we have explored a new hypothetical Pn-based clathrate family from the density functional calculations. Such a family with a general formula of $A_8B_xPn_{46-x}$ (A = alkali or alkaline-earth metal; B = group 11 or 12 element; Pn = pnicogen) is especially interesting because their Pn-based frameworks are different from the well-known type-I Tt-based clathrate in several aspects, such as site preference and atomic distribution. The stabilities of the Pn-based clathrates are evaluated by the formation energies. The transport properties of some of the energetically favorable compounds are estimated based on the Boltzmann transport equation.[20,21] The results in this paper are hoped to provide a guidance for the ongoing experimental works.

Method and Models

The density functional calculations were performed by the Vienna *ab initio* simulation package VASP.[22] We used a plane wave basis with the projector augmented wave (PAW)[23,24] potentials. First, the local-density approximation (LDA) was used in the structure optimizations. A plane wave cut off energy of 273, 250, 277, and 274 eV were set for Cu-, Ag-, Zn-, and Cd-containing compounds, respectively. After collecting the data that contain the energies for different lattice parameters, we fit the energy to the Birch−Murnaghan equation of state (EOS)[25] to obtain the equilibrium volume and the bulk modulus. Then, the generalized gradient approximation (GGA) was used to calculate the total energy and band structure. The corresponding cut off energies were 368, 250, 274, and 277 eV for Cu-, Ag-, Cd-, and Zn-containing compounds, respectively. For DOS calculations, we used a $4 \times 4 \times 4$ Monkhorst−Pack k-point grid within the Brillouin zone. The transport properties should be calculated with very large k-points in the irreducible Brillouin

(14) Burdett, J. K.; Canadell, E. *J. Am. Chem. Soc.* **1990**, *112*, 7207–7217.
(15) Burdett, J. K.; Lee, S. *J. Am. Chem. Soc.* **1985**, *107*, 3050–3063.
(16) Burdett, J. K.; Lee, S. *J. Am. Chem. Soc.* **1985**, *107*, 3063–3082.
(17) Blake, N. P.; Latturner, S.; Bryan, J. D.; Stucky, G. D.; Metiu, H. *J. Chem. Phys.* **2001**, *115*, 8060–8073.
(18) Martin, J.; Erickson, S.; Nolas, G. S.; Alboni, P.; Tritt, T. M.; Yang, J. *J. Appl. Phys.* **2006**, *99*, 044903.
(19) Martin, J.; Nolas, G. S.; Wang, H.; Yang, J. *J. Appl. Phys.* **2007**, *102*, 103719.
(20) Allen, P. B. Boltzmann Theory and Resistivity of Metals. In Quantum Theory of Real Materials;Chelikowsky, J. R., Louie, S. G., Eds.; Kluwer: Boston, MA, **1996**; Chapter 17, pp 219−250.
(21) Bronold, F. X. Boltzmann Transport in Condensed Matter. In Computational Many-Particle Physics; Caron, C., Ed.; Springer: Berlin, Germany, **2008**; Vol. *739*, pp 223−254.
(22) Kresse, G.; Furthmuller, J. *Phys. Rev. B* **1996**, *54*, 11169–11186.
(23) Kresse, G.; Joubert, D. *Phys. Rev. B* **1999**, *59*, 1758–1775.
(24) Blochl, P. E. *Phys. Rev. B* **1994**, *50*, 17953–17979.
(25) Birch, F. *Phys. Rev.* **1947**, *71*, 809–824.

zone (IBZ). However, because of the complexity of the type-I clathrate structure, a $7 \times 7 \times 7$ k-point grid (172 k-points in IBZ) was used which gave compatible results to a $8 \times 8 \times 8$ grid (256 k-points in IBZ) that needed more than 24-gigabyte memory. The Seebeck coefficient and electrical conductivity were calculated using the BoltzTraP package written by Madsen.[26] The Boltzmann equation was used to describe the change of the carrier distribution in the real materials. Nevertheless, it was hard to obtain an exact solution of the Boltzmann equation because of the complexity of the carrier scattering. Often, in practice, the relaxation time τ was assumed a constant value that is energy- and direction-independent. Such a simple assumption gave a good approximation to evaluate the transport properties in some thermoelectric compounds.[17,27−30] Then the Seebeck coefficient could be calculated by eq 1.

$$S(T,\mu) = \frac{1}{eT\sigma(T,\mu)} \int \sigma_{\alpha\beta}(\varepsilon)(\varepsilon-\mu)\left[-\frac{\partial f_\mu(T,\varepsilon)}{\partial \varepsilon}\right] \mathrm{d}\varepsilon \quad (1)$$

where T, e, and μ were temperature, electron charge, and chemical potential, respectively. The α and β were tensor indices. The electrical conduction σ and the conductivity distribution $\sigma_{\alpha\beta}$ were written as eqs 2 and 3, respectively.

$$\sigma(T,\mu) = \frac{1}{\Omega} \int \sigma_{\alpha\beta}(\varepsilon)\left[-\frac{\partial f_\mu(T,\varepsilon)}{\partial \varepsilon}\right] \mathrm{d}\varepsilon \quad (2)$$

and

$$\sigma_{\alpha\beta}(\varepsilon) = \frac{e^2}{N} \sum_{i,\mathbf{k}} \tau v_\alpha(i,\mathbf{k}) v_\beta(i,\mathbf{k}) \frac{\delta(\varepsilon-\varepsilon_{i,\mathbf{k}})}{\mathrm{d}\varepsilon} \quad (3)$$

where N, Ω, and $\varepsilon_{i,\mathbf{k}}$ were the number of $\mathbf{k}$ points sampled, the volume of the unit cell, and the band energy of the ith band with a wave vector $\mathbf{k}$. The group velocity $v(i,\mathbf{k})$ was evaluated from the band structure by eq 4.

$$v(i,\mathbf{k}) = \frac{1}{\hbar} \frac{\partial \varepsilon_{i,\mathbf{k}}}{\partial \mathbf{k}} \quad (4)$$

The rigid band approach (RBA)[31,32] was another assumption used to evaluate the Seebeck coefficient and the power factor. On the basis of this assumption, the Fermi energy would be shifted up or down to modify the carrier concentration without changing any other feature of the corresponding band structure.

Results and Discussion

Stoichiometry of a Possible Tetrel- or Pnicogen-Based Type-I Clathrate Containing a Group 11 or 12 Element. Compounds with general formula of $A_8B_xC_{46-x}$ constructed by tetrel or pnicogen atoms together with group 11 (Cu, Ag) or group 12 (Zn, Cd) elements are considered. We have listed all the possible stoichiometries in Table 1 based on the following assumptions: (1) No vacancy on the framework has been considered. (2) All the structures discussed will be retained in a cubic symmetry, since the unit cell of a real clathrate may be crystallographically approximated as an average cubic unit cell.[17,43]

For a type-I clathrate, the frame atoms, B and C, are 4-fold bonded and the guest ion A should provide enough electrons to balance the charge requirement of the framework. Therefore, the number of B atoms (x) can be calculated according to the inequality (eq 5):

$$(4-B_{\mathrm{ox}})x - (C_{\mathrm{ox}}-4)(46-x) \le 8A_{\mathrm{ox}} \quad (5)$$

where B_{ox} is the number of valence electrons of B, (B = group 11, 12 or triel; $B_{\mathrm{ox}} = 1$, 2, or 3), and C_{ox} is the number of valence electrons of C, (C = tetrel or pnicogen; $C_{\mathrm{ox}} = 4$ or 5). A is defined as alkali-metal (K, Rb, Cs; $A_{\mathrm{ox}} = 1$) or alkaline-earth metal (Sr, Ba; $A_{\mathrm{ox}} = 2$). Note that we have not considered the inverse examples, such as $Ge_{38}Sb_8I_8$, $Sn_{38}Sb_8I_8$, and $Ge_{30}P_{16}Te_8$,[33,34] in which A can be a halogen (Br, I; $A_{\mathrm{ox}} = -1$) or chalcogen (Te; $A_{\mathrm{ox}} = -2$). We also have not considered another case with $B_{\mathrm{ox}} = 3$ and $C_{\mathrm{ox}} = 4$, which are constructed by both tetrels (Si, Ge, Sn) and triels (B, Al, Ga, In), for example, $A_8B_8C_{38}$ (A = K, Rb, Cs; B = Al, Ga, In; C = Ge, Sn)[35] and (Ba or Sr)$_8$Ga$_x$(Ge, Si, or Sn)$_{46-x}$ (x = 4.44, 8.62, 11.95, 12.35, 13.82, 16, etc.).[4,36,40]

Table 1 lists all the possible Pn-based type-I clathrates that are containing group 11 or 12 elements. For clarity, we use class-I to represent $A_8B_xPn_{46-x}$ (B = group 11; $12 \le x \le 15$) and class-II for $A_8B_xPn_{46-x}$ (B = group 12; $16 \le x \le 20$), wherein, A = alkali- or alkaline-earth metal; Pn = pnicogen. Table 1 also lists all the possible Tt-based type-I clathrates that are containing group 11 or 12 elements as $A_8B_xTt_{46-x}$ (A = alkali-metal or alkaline-earth; B = group 11 or 12; $1 \le x \le 8$; Tt = tetrel). In the following sections, in order to minimize the computational calculations, we have limited the constituents within the selected elements: Cs, Ba; Cu, Ag; Zn, Cd; and Sb. As listed in Table 1, several Tt-based clathrates containing group 11 or 12 examples are known, such as $Ba_8Cu_{6-x}Ge_{40+x}$ ($0 \le x \le 0.7$),[7] $Ba_8Zn_8Ge_{38}$,[9,41]

(26) Madsen, G. K. H.; Singh, D. J. *Comput. Phys. Commun.* **2006**, *175*, 67–71.
(27) Qiu, A. N.; Zhang, L. T.; Shan, A. D.; Wu, J. S. *Phys. Rev. B* **2008**, *77*, 205207.
(28) Yang, J.; Li, H. M.; Wu, T.; Zhang, W. Q.; Chen, L. D.; Yang, J. H. *Adv. Funct. Mater.* **2008**, *18*, 2880–2888.
(29) Iversen, B. B.; Palmqvist, A. E. C.; Cox, D. E.; Nolas, G. S.; Stucky, G. D.; Blake, N. P.; Metiu, H. *J. Solid State Chem.* **2000**, *149*, 455–458.
(30) Blake, N. P.; Mollnitz, L.; Kresse, G.; Metiu, H. *J. Chem. Phys.* **1999**, *111*, 3133–3144.
(31) Kidron, A. *Phys. Rev. Lett.* **1969**, *22*, 774–776.
(32) Stern, E. A. *Phys. Rev.* **1967**, *157*, 544–551.
(33) Schnering, H. G. v.; Menke, H. *Z. Anorg. Allg. Chem.* **1976**, *424*, 108–114.
(34) (a) Kishimoto, K.; Arimura, S.; Koyanagi, T. *Appl. Phys. Lett.* **2006**, *88*, 22215. (b) Kishimoto, K.; Arimura, S.; Koyanagi, T. *Appl. Phys. Lett.* **2006**, *89*, 172106.
(35) Kröner, R.; Peters, K.; Schnering, H. G. v.; Nesper, R. *Z. Kristallogr.-New Cryst. Struct.* **1998**, *213*, 667–675.
(36) (a) Suekuni, K.; Avila, M. A.; Umeo, K.; Fukuoka, H.; Yamanaka, S.; Nakagawa, T.; Takabatake, T. *Phys. Rev. B* **2008**, *77*, 235119. (b) Carrillo-Cabrera, W.; Gil, R. C.; Grin, Y. Z. *Kristallogr.-New Cryst. Struct.* **2002**, *217*, 179–180. (c) Carrillo-Cabrera, W.; Gil, R. C.; Tran, V.-H.; Grin, Y. Z. *Kristallogr. -New Cryst. Struct.* **2002**, *217*, 181–182. (d) Carrillo-Cabrera, W.; Gil, R. C.; Paschen, S.; Grin, Y. Z. *Kristallogr.-New Cryst. Struct.* **2002**, *217*, 183–185.

Table 1. Hypothetical $A_8B_xC_{46-x}$ Compounds[a]

n_B	B_{ox} +1	known example	B_{ox} +2	known example
1	$(I \text{ or } II)_8(IB)_1(IV)_{45}$		$(I \text{ or } II)_8(IIB)_1(IV)_{45}$	
2	$(I \text{ or } II)_8(IB)_2(IV)_{44}$		$(I \text{ or } II)_8(IIB)_2(IV)_{44}$	
3	$(I \text{ or } II)_8(IB)_3(IV)_{43}$	$Ba_8Cu_{6-x}Ge_{40+x}$[b] ($0 \le x \le 0.7$)	$(I \text{ or } II)_8(IIB)_3(IV)_{43}$	$Ba_8Cd_8Ge_{38}$[c]
4	$(II)_8(IB)_4(IV)_{42}$		$(I \text{ or } II)_8(IIB)_4(IV)_{42}$	$Ba_8Zn_8Ge_{38}$[c,d]
5	$(II)_8(IB)_5(IV)_{41}$		$(II)_8(IIB)_5(IV)_{41}$	$Sr_8Zn_8Ge_{38}$[e]
6			$(II)_8(IIB)_6(IV)_{40}$	$Rb_8Hg_4Sn_{42}$[f]
7			$(II)_8(IIB)_7(IV)_{39}$	
8			$(II)_8(IIB)_8(IV)_{38}$	
9				
10				
11				
class-I			class-II	
12	$(I \text{ or } II)_8(IB)_{12}(V)_{34}$			
13	$(I \text{ or } II)_8(IB)_{13}(V)_{33}$			
14	$(II)_8(IB)_{14}(V)_{32}$			
15	$(II)_8(IB)_{15}(V)_{31}$			
16			$(I \text{ or } II)_8(IIB)_{16}(V)_{30}$	
17			$(I \text{ or } II)_8(IIB)_{17}(V)_{29}$	
18			$(I \text{ or } II)_8(IIB)_{18}(V)_{28}$	$Cs_8(Cd \text{ or } Zn)_{18}Sb_{28}$[g]
19			$(II)_8(IIB)_{19}(V)_{27}$	
20			$(II)_8(IIB)_{20}(V)_{26}$	

[a] A represents alkali-metal or alkaline-earth metal; B is group 11 or group 12 element, and C means tetrel or pnicogen. The term n_B and B_{ox} are the number of B elements and the number of valence electrons, respectively. The available real compounds are also listed. I = alkali-metal; II = alkaline-earth metal; IB = group 11; IIB = group 12; IV = tetrel; V = pnicogen. [b] From ref 7. [c] From ref 41. [d] From ref 9. [e] From ref 40. [f] From ref 52. [g] From ref 42

$Ba_8Cd_8Ge_{38}$,[37,41] $Cs_8Cd_4Sn_{42}$,[38] $Cs_8Zn_4Sn_{42}$,[39] and $Rb_8Hg_4Sn_{42}$,[52] which fit in the inequality (eq 5). Only two Pn-based clathrates containing group 11 or 12 of $Cs_8Zn_{18}Sb_{28}$ and $Cs_8Cd_{18}Sb_{28}$[42] have been synthesized so far. We will discuss the stability of the hypothetical group 11-Sb- or group 12-Sb-based clathrates as listed in Table 1. The formation energy, unit cell parameter, band gap, site configuration of a certain stoichiometry, as well as the site preference of Zn and Cd are studied. Note that $A_8B_xTt_{46-x}$ (B = group 11 or 12) is not intended because it can be treated as a group 11 or 12 doped Tt-based clathrate, which belongs to the category of the Tt-based type-I clathrates (Tt = Si, Ge, or Sn).

Formation Energy of the Group 11 (Cu, Ag)-Sb- or Group 12 (Zn, Cd)-Sb-Based Clathrate. Since $Ba_8Ga_{16}Ge_{30}$ has significant thermoelectric property, any new type-I clathrate will be surveyed for its thermoelectric property. However, the available data are limited; only two Sb-based Zn and Cd containing clathrates have been synthesized so far. Therefore, the possible formation and the stability of a new Sb-based clathrate are of great interest. We have therefore calculated the formation energies of the Sb-based clathrates listed in Table 1. Similar as previous studies,[3,43] the formation energy is defined as the total energy difference between the hypothetical compound and its corresponding isolate bulk constituent elements, as eq 6 indicated:

$$E_f(A_8B_xC_{46-x}) = E_{A_8B_xC_{46-x}} - 8E_A - xE_B - (46-x)E_C \quad (6)$$

The stoichiometry is taken from Table 1. The site configuration revealing the frame atom identity and the number of atom on each site (6*c*, 16*i*, or 24*k* sites) is set according to that in $Ba_8Ga_{16}Ge_{30}$.[3,43] For example, experimental and theoretical studies show that, in the most energetically stable site configuration of $Ba_8Ga_{16}Ge_{30}$, Ga atoms have taken 3 6*c* sites, 1 16*i* site, and 12 24*k* sites, in which no Ga−Ga bond is formed.[3,43] We have denoted hereafter such a site configuration as (3, 1, 12). Assuming Cu and Ag have the similar site preference as Ga, then, the site configuration of $Ba_8Cu_{14}Sb_{32}$ will be denoted as (3, 1, 10) (Table 2, column 3), which means three Cu will sit on the 6*c* site and one on the 16*i*, and ten Cu atoms on the 24*k* site. Subsequently, six hypothetical compounds have been selected to calculate the cell parameters, bulk moduli, formation energies per atom, as well as the band gaps (Table 2). The calculations indicate that, with the same stoichiometry and site configuration, the unit cell parameter for Ag-clathrate is larger than that of Cu-clathrate, because Ag has a larger covalent radius than the Cu atom. Similarly, the cell parameters slightly decrease as the increase of the percentage of Cu or Ag, because the covalent radius for Cu and Ag are slightly smaller than that of Sb atoms. For comparison, the formation energies of $Cs_8B_{14}Sb_{32}$ (B = Cu, Ag) that do not obey the inequality in eq 5 are also calculated. The positive formation energy of the electron-poor $Cs_8Cu_{14}Sb_{32}$ suggests that it is thermodynamically unstable. $Cs_8Ag_{14}Sb_{32}$ also disobeys eq 5, but it is slightly thermodynamically stable. Yet, $Cs_8Ag_{14}Sb_{32}$ may be unstable because its formation

(37) Czybulka, A.; Kuhl, B.; Schuster, H. U. *Z. Anorg. Allg. Chem.* **1991**, *594*, 23–28.
(38) Wilkinson, A. P.; Lind, C.; Young, R. A.; Shastri, S. D.; Lee, P. L.; Nolas, G. S. *Chem. Mater.* **2002**, *14*, 1300–1305.
(39) Nolas, G. S.; Chakoumakos, B. C.; Mahieu, B.; Long, G. J.; Weakley, T. J. R. *Chem. Mater.* **2000**, *12*, 1947–1953.
(40) Qiu, L. Y.; Swainson, I. P.; Nolas, G. S.; White, M. A. *Phys. Rev. B* **2004**, *70*, 035208.
(41) Kuhl, B.; Czybulka, A.; Schuster, H. U. *Z. Anorg. Allg. Chem.* **1995**, *621*, 1–6.
(42) Liu, Y.; Wu, L.-M.; Li, L.-H.; Du, S.-W.; Corbett, J. D.; Chen, L. *Angew. Chem., Int. Ed.* **2009**, *48*, 5305–5308.
(43) Emmanuel, N. N.; Charles, W. M. *Phys. Rev. B* **2008**, *77*, 205203.

Table 2. Some Class-I Hypothetical Compounds $A_8B_xSb_{46-x}$[a]

B_{ox}	cell parameter	site configuration					
+1	a (Å)	6*c*	16*i*	24*k*	E_f (eV/atom)	bulk modulus (Gpa)	band gap (eV)
$Ba_8Cu_{14}Sb_{32}$	11.575	3	1	10	−0.1070	51.3	
$Ba_8Ag_{14}Sb_{32}$	11.846				−0.1922	50.9	
$Ba_8Cu_{15}Sb_{31}$	11.496	3	1	11	−0.1296	53.5	
$Ba_8Ag_{15}Sb_{31}$	11.789				−0.2062	52.7	
$Na_2Ba_6Cu_{15}Sb_{31}$	11.480				−0.0687	53.1	
$Na_2Ba_6Ag_{15}Sb_{31}$	11.772				−0.1413	50.9	
examples disobey inequality in eq 5:							
$Cs_8Cu_{14}Sb_{32}$	11.666	3	1	10	0.0099	45.1	
$Cs_8Ag_{14}Sb_{32}$	11.948				−0.0976	44.9	

[a] A = Ba, Cs, Na; B = Cu or Ag; $12 \le x \le 15$. The calculated formation energy (eV/atom), cell parameter (Å), bulk modulus (GPa), and band gap (eV). Hypothetical compounds $Cs_8Cu_{14}Sb_{32}$ and $Cs_8Ag_{14}Sb_{32}$ that disobey the inequality (eq 5) are also listed.

Table 3. Some Class-II Hypothetical Compounds $A_8B_xSb_{46-x}$[a]

B_{ox}	cell parameter	site configuration					
+2	a (Å)	6*c*	16*i*	24*k*	E_f (eV/atom)	bulk modulus (GPa)	band gap (eV)
$Ba_8Cd_{16}Sb_{30}$	12.101	3	1	12	−0.2246	42.2	
$Ba_8Zn_{16}Sb_{30}$	11.732				−0.1979	43.8	
$Cs_8Cd_{16}Sb_{30}$	12.172				−0.2112	38.8	
$Cs_8Zn_{16}Sb_{30}$	11.797				−0.1628	40.1	
$Ba_8Cd_{18}Sb_{28}$	12.036	3	1	14	−0.2293	42.8	
$Ba_8Zn_{18}Sb_{28}$	11.620	3	1	14	−0.2036	44.8	
$Cs_8Cd_{18}Sb_{28}$	12.120; 12.192[b]	3	1	14	−0.1971	39.0 (2)	
	12.162	3	4	11	−0.1775	37.2 (5)	
	12.116	3	6	9	−0.1967	38.9 (4)	
	12.169	3	12	3	−0.1582	37.9 (6)	
	12.147	1	1	16	−0.1778	38.2 (2)	
	12.115	1	3	14	−0.1958	38.6 (0)	
	12.141	4	1	13	−0.1859	37.6 (5)	
$Cs_8Zn_{18}Sb_{28}$	11.694; 11.705[b]	3	1	14	−0.1495	41.2	
	11.748	3	4	11	−0.1203	40.6	
	11.682	3	6	9	−0.1543	42.8	
	11.756	3	12	3	−0.1019	40.8	
	11.734	1	1	16	−0.1228	42.0	
	11.686	1	3	14	−0.1506	43.0	semimetal
	11.732	4	1	13	−0.1294	41.3	
$Cs_8Cd_{20}Sb_{26}$[c]	12.076	3	2	15	−0.1880	39.7	
$Ba_8Cd_{20}Sb_{26}$	11.971				−0.2390	43.9	
$Ba_8Zn_{20}Sb_{26}$	11.512				−0.2278	47.6	
$Na_2Ba_6Cd_{20}Sb_{26}$	11.959				−0.1877	43.0	
$Na_2Ba_6Zn_{20}Sb_{26}$	11.494				−0.1796	46.4	
$Sr_8Ga_{16}Ge_{30}$	10.559; 10.727[d]	3	1	12	−0.280; −0.301[d]	67.7; 64.0[e]	0.28;0.18[f]
$Ba_8Ga_{16}Ge_{30}$	10.629; 10.764[d]	3	1	12	−0.373; −0.387[d]	66.5; 65.3[e]	0.53;0.55[f]

[a] (A = Ba, Cs, Na; B = Zn or Cd; $16 \le x \le 20$). The calculated formation energy (eV/atom), cell parameter (Å), bulk modulus (GPa), and band gap (eV) for different B (Cd or Zn) site configurations in the lattice. Compounds $Ba_8Ga_{16}Ge_{30}$ and $Sr_8Ga_{16}Ge_{30}$ are also listed for comparison. [b] From ref 42. [c] Example disobeys the inequality in eq 5. [d] From ref 3. [e] From ref 41. [f] From ref 43.

energy, −0.0976 eV/atom, is almost 100 meV/atom higher than the inequality-obeyed $Ba_8Ag_{14}Sb_{32}$. In general, the formation energies for the Cu-analogues are about 0.4 times higher than that of the Ag-analogues and thus Ag-analogues should be more thermodynamically stable than the Cu-analogues. The two $Na_2Ba_6B_{15}Sb_{31}$ (B = Cu, Ag) examples also suggest that the introduction of Na decreases the stability of $Ba_8B_xSb_{46-x}$ (B = Cu, Ag, $x = 14$, 15). These class-I compounds are metallic, and the detailed discussions on the band structures are presented below.

We have also calculated class-II compounds, $A_8B_xSb_{46-x}$ (A = Ba, Cs, and Na + Ba; B = Cd, Zn; $x = 16$, 18, 20), the formation energy, cell parameter, bulk modulus, and band gap are listed in Table 3. The calculated and experimental cell parameters of $Ba_8Ga_{16}Ge_{30}$, $Sr_8Ga_{16}Ge_{30}$, $Cs_8Cd_{18}Sb_{28}$, and $Cs_8Zn_{18}Sb_{28}$ are consistent.[4,42] The bulk moduli for $Ba_8Ga_{16}Ge_{30}$ and $Sr_8Ga_{16}Ge_{30}$ fitted by the Birch−Murnaghan equation of state are consistent with the experimental data.[44] The calculated formation energies for $Ba_8Ga_{16}Ge_{30}$ and $Sr_8Ga_{16}Ge_{30}$ are similar to the values reported.[3] Therefore, the data in Tables 2 and 3 should be reliable.

On the basis of these results, the absolute formation energies for Ba-analogues increase with the increase of the Cd or Zn content, while the absolute formation energies for Cs-analogues decrease. Although disobeying the inequality in eq 5, electron-poor $Cs_8Cd_{20}Sb_{26}$ is energetically favorable. Similar as those listed in Table 2, the substitute of Ba by Na in $Ba_8B_{20}Sb_{26}$ (B = Cd, Zn) leads to a stability decrease. In general, with same frame-constituent and site configuration, the

(44) Okamoto, N. L.; Nakano, T.; Tanaka, K.; Inui, H. *J. Appl. Phys. Lett.* **2008**, *104*, 013529.

Table 4. Site Configuration, Type of Bond, and Number of Bonds[a]

site configuration	inner-cell		intracell	
6*c*, 16*i*, 24*k*	Cd−Cd or Zn−Zn	Ext-(Cd−Cd) or Ext-(Zn−Zn)	Cd−Cd or Zn−Zn	total nb
(3, 1, 14)	(6*c*-24*k*) × 2	0	(24*k*-24*k*) × 2	4
(3, 4, 11)	(6*c*-24*k*) × 1 (16*i*-24*k*) × 2	(24*k*-16*i*-24*k*) × 1	(24*k*-24*k*) × 2	7
(3, 6, 9)	(16*i*-24*k*) × 2	(24*k*-16*i*-24*k*) × 1	0	4
(3, 12, 3)	(16*i*-24*k*) × 1 (16*i*-16*i*) × 2	(16*i*-16*i*-24*k*-16*i*-16*i*) × 1	0	7
(4, 1, 13)	(6*c*-24*k*) × 2	(6*c*-(24k)$_3$) × 1	(24*k*-24*k*) × 2	7
(1, 1, 16)	(6*c*-24*k*) × 1 (24*k*-24*k*) × 1	0	(24*k*-24*k*) × 6	8
(1, 3, 14)	(16i-24k) × 1	0	(24*k*-24*k*) × 4	5

[a] The bonds include the $M_{site}-M_{site}$ (M is Cd or Zn; site contains 6*c*, 16*i*, and 24*k*) bonds lying in the unit cell (inner-cell) and those between two unit cells (intracell) as well as the "continuous Cd−Cd or Zn−Zn bonds" in the unit cell denoted as Ext-(Cd−Cd) or Ext-(Zn−Zn). Total nb is the total number of Cd−Cd or Zn−Zn bonds in the unit cell. The figures of the $M_{site}-M_{site}$ bonds of each configuration are shown in the Supporting Information (Figure S3).

stability trend is as follows: $Ba_8B_xSb_{46-x} > Cs_8B_xSb_{46-x}$ and $A_8Cd_xSb_{46-x} > A_8Zn_xSb_{46-x}$. Such an observation suggests that the hypothetical $Ba_8Cd_xSb_{46-x}$ ($16 \le x \le 20$) is energetically favorable and is worth trying.

Stability studies have found that (1) Ag(Cd)-analogues should be more thermodynamically stable than Cu(Zn)-analogues. (2) The absolute formation energies for Ba-analogues increase with the Cd or Zn content, whereas those for Cs-analogues decrease. (3) The replacement of Ba by Na results in a stability decrease in class I (Cu- or Ag−Sb-framework) as well as in class II (Zn- or Cd−Sb-framework). (4) The electron-poor group 12-Sb framework is more stable than the electron-poor group 11-Sb framework.

Site Preference of Zn or Cd in a Sb-Based Clathrate. As briefly mentioned above, the type-I clathrate compound has a 3D complicated framework that is constructed by two kinds of polyhedra, 24-atom tetrakaidecahedron and 20-atom dodecahedron, which are defined by three distinctive crystallographic sites: 6*c*, 16*i*, and 24*k*. For a heteroelement framework, the sitting of the atom on the different frame sites may show a site-preference as found in $Ba_8Ga_{16}Ge_{30}$, in which the 16 Ga atoms have been distributed as 3 on 6*c* sites, 1 on the 16*i* site, and 12 on 24*k* sites.[3] Note that the sitting of element, or so-called "coloring problem",[12,13] is of great importance because it will eventually determine the stoichiometry of a compound, cause the fractional occupancy on each crystallographic site, as well as arise the disorder of different elements on the same site, and so on. These problems inevitably give great troubles to the syntheses and the crystallographic refinements. Unfortunately, the site configuration of a clathrate that does not contain Ge is unclear up to now. We, therefore, calculated the cell parameters and the formation energies for several Sb-based clathrates containing Cd or Zn with different site configurations (Table 3). For some selected site configurations, the number of $M_{site}-M_{site}$ bonds (M = Cd, or Zn; sites are 6*c*, 16*i*, and 24*k*) is presented in Table 4. The relationship between formation energy and site configuration is plotted in Figure 2. Our calculation results confirm that the group 12-group 12 bond is not advantageous to the stability of a clathrate. Take a certain compound $Cs_8Cd_{18}Sb_{28}$ for instance, the site configurations (3, 12, 3), (3, 4, 11), and (4, 1, 13) have 7 Cd−Cd bonds and (1, 1, 16), 8 Cd−Cd bonds. These four configurations exhibit

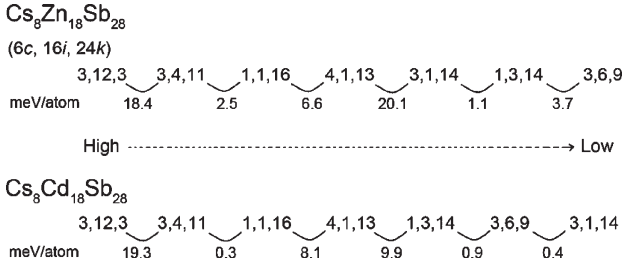

Figure 2. Formation energy sequence for $Cs_8Zn_{18}Sb_{28}$ and $Cs_8Cd_{18}Sb_{28}$ with different site configurations. For each sequence, the upper figures represent the site configurations and the lower numbers represent the formation energy difference between the two neighboring configurations.

formation energies at least 9.9 meV/atom higher than the formation energies for other site configurations with less Cd−Cd bonds, such as (3, 1, 14), (3, 6, 9), 4 Cd−Cd bonds; and (1, 3, 14), 5 Cd−Cd bonds. Such a group 12-group 12 bond number-related formation energy difference is significantly large for the corresponding Zn-analogues, e.g., the two configurations (4, 1, 13) and (3, 1, 14) of Zn-analogue has a 20.1 meV/atom difference in energy (Figure 2). Other compounds also disfavor the group 12-group 12 bond, e.g., β-Zn_4Sb_3[45] and $Mn_8Ga_{27.4}Zn_{13.6}$.[46]

Figure 2 also indicates that E_f orders of configurations with larger numbers of group 12-group 12 bonds (e.g., (3, 12, 3); (3, 4, 11); (1, 1, 16); (4, 1, 13)) for $Cs_8Cd_{18}Sb_{28}$ and $Cs_8Zn_{18}Sb_{28}$ are the same but different for those with fewer numbers of bonds (e.g., (3, 1, 14); (1, 3, 14); (3, 6, 9)). For example, the most stable site configuration for $Cs_8Zn_{18}Sb_{28}$ is (3, 6, 9), while for $Cs_8Cd_{18}Sb_{28}$, it is (3, 1, 14). Besides, $Cs_8Zn_{18}Sb_{28}$-(1, 3, 14) is 1.1 meV/atom lower than $Cs_8Zn_{18}Sb_{28}$-(3, 1, 14). While in $Cs_8Cd_{18}Sb_{28}$, these two configurations show opposite energy order: $Cs_8Cd_{18}Sb_{28}$-(3, 1, 14) is 1.3 meV/atom lower than $Cs_8Cd_{18}Sb_{28}$-(1, 3, 14). How shall we explain such a deviation? The possible reason is that the 16*i*-site prefers Zn to Cd, while the 6*c*-site prefers Cd to Zn. Such a site preference-difference may due to the different site geometry and covalent radius. As indicated in Figure 1c, on the six-membered ring of $Cs_8Cd_{18}Sb_{28}$, the on-plane-angle is 110.8° around the 6*c* site (24*k*-6*c*-24*k*) and 124.6° around the 24*k* site

(45) Nylen, J.; Lidin, S.; Andersson, M.; Iversen, B. B.; Liu, H. X.; Newman, N.; Haussermann, U. *Chem. Mater.* **2007**, *19*, 834–838.
(46) Haussermann, U.; Viklund, P.; Svensson, C.; Eriksson, S.; Berastegui, P.; Lidin, S. *Angew. Chem., Int. Ed.* **1999**, *38*, 488–492.

(6*c*-24*k*-24*k*), while the off-plane-angles range from 105.3 to 108.8° for both sites. If an atom with small radius occupies the sites on such a ring, its coordination sphere will bear great distortion and it will endure pronounced stress. In comparison, a large atom on the ring should have less stress.[49] Thus, a large atom prefers sites on the six-membered ring. Such a radius-dependent site preference has also been found in $Ba_8Al_{14}Si_{31}$[47,48] and $K_7B_7Si_{39}$,[49] in which the 6*c* site on the six-membered ring have a very low occupancy of small Al or B while the 16*i* site is partially occupied by Al or B. This is different from the Tt-based heavy Tr containing clathrates, such as $Ba_8Ga_{16}Si_{30}$, $Ba_8Ga_{16}Ge_{30}$, and $Ba_8In_{16}Ge_{30}$, in which the 6*c* site on the six-membered ring shows a large occupancy of Ga or In.[4] Similarly, the 6*c* and 24*k* sites on the six-membered ring prefer Cd to Zn. Furthermore, the Tt element has the first priority to occupy the 16*i* sites. If a clathrate does not contain any Tt element, its 16*i* site will prefer a small atom. For example, with the same number of Zn−Zn or Cd−Cd bonds, $Cs_8Zn_{18}Sb_{28}$-(3, 6, 9) is more stable than $Cs_8Zn_{18}Sb_{28}$-(3, 1, 14) by 4.8 meV/atom; however, the formation energy difference between $Cs_8Cd_{18}Sb_{28}$-(3, 6, 9) and $Cs_8Cd_{18}Sb_{28}$-(3, 1, 14) is only 0.4 meV/atom (Figure 2), which indicates that the 16*i* sites accommodate more Zn than Cd. Consequently, with the same number of group 12−group 12 bonds, the stable configuration of the Zn−Sb framework should distribute Zn as least as possible on the six-membered ring sites and as more as possible on the 16*i*-site. In contrast, the stable configuration of the Cd−Sb framework should accommodate Cd as much as possible on the six-membered ring sites. We, then, can understand why $Cs_8Zn_{18}Sb_{28}$-(3, 6, 9) and $Cs_8Cd_{18}Sb_{28}$-(3, 1, 14) are the most stable configurations. Also, $Cs_8Zn_{18}Sb_{28}$-(1, 3, 14) and $Cs_8Cd_{18}Sb_{28}$-(3, 1, 14) are more stable than $Cs_8Zn_{18}Sb_{28}$-(3, 1, 14) and $Cs_8Cd_{18}Sb_{28}$-(1, 3, 14), respectively. These observations seem to agree with the experimental data. The single crystal diffraction data indicate that 6*c* sites in $Cs_8Cd_{18}Sb_{28}$ are fully occupied by Cd and 16*i* sites do not contain any Cd, which gives a configuration of (6, 0, 12); while the 6*c* and 16*i* sites in $Cs_8Zn_{18}Sb_{28}$ are occupied by three Zn, which generate a configuration of (3, 3, 12).[42] The formation energies of these two configurations have been calculated. The $Cs_8Cd_{18}Sb_{28}$-(6, 0, 12) with 10 Cd−Cd bonds has a relatively high formation energy of −0.1348 eV/atom. Also, $Cs_8Zn_{18}Sb_{28}$-(3, 3, 12) with 4 Zn−Zn bonds has a formation energy of −0.1449 eV/atom, which is comparable to that of (3, 1, 14) listed in Table 3.

Now back to our first question set in the Introduction: Will the site preference on a Pn-based framework be similar to that on the Tt-based framework? Briefly, the major differences between them are (1) unlike Ga in a Ga−Ge framework that avoids the 16*i* site, Cd and Zn do not disfavor the 16*i* site. (2) Tt element has the first priority to occupy the 16*i* site. Pn-based clathrate does not contain any Tt element, its 16*i* site prefers a small atom, i.e., the 16*i* site prefers Zn to Cd. On the other hand, these two kinds of clathrates share some common characteristics: (1) a stable Pn- or Tt-based clathrate always prefers a group 12−group 12 bond or a Ga−Ga bond at least. (2) If an atom sits on the six-membered ring of a Pn- or Tt-based clathrate, the smaller the atom is, the larger distortion it bears, the higher stress it endures, and the more unstable the structure is.

However, the calculations described above do not provide a complete understanding of the configuration−energy relationship. One possibility is that the formation energy is determined by both the number of group 12−group 12 bond and group 12−Sb bond. For example, configurations of (3, 4, 11) and (4, 1, 13) have the same number of Cd−Cd or Zn−Zn bonds, but their formation energies are different because the bond binding energies of $M_{6c}-M_{24k}$ and $M_{16i}-M_{24k}$ are different owing to the different bond lengths and coordination spheres. The formation energies listed in Tables 2 and 3 also show that the larger the lattice is, the less stable the compound is. Of course, the $M_{site}-M_{site}$ binding energy will aid further understanding of the structure−energy relationship of a clathrate; however, such data are not available at present. The reason is that long-distance or secondary interactions in a solid-state crystal system are important, and even we can roughly evaluate the $M_{site}-M_{site}$ binding energy via the energy loss when one Cd or Zn atom is removed from the frame sites; in fact, we have not yet found a suitable way to precisely calculate the $M_{site}-M_{site}$ binding energy.

Band Structures and Electronic Transport Properties. Here, we will explore the electronic structures and transport properties of Cu/Ag−Sb- and Zn/Cd)-Sb-clathrates to answer the second question we set in the Introduction. The band structures for class-I hypothetical compounds listed in Table 2 are plotted in Figure 3. The inclusion of Cu 3p states has an unnoticeable effect on the band structures. All these compounds are metallic, and the features of their band structures are new. In Ag−Sb- or Cu−Sb-clathrate, the guest Ba atom plays a different role from that in Ga−Ge-clathrates. The wave functional character has been calculated to figure out how many states coming from Ba and how many states from the frame atoms that participate in each selected band. The wave functional character is calculated via projecting the wave functionals onto the spherical harmonics within spheres around each ion (P_{Nlnk}), and the *l*-quantum (s, p, d) of each ion is represented by the participation proportion in each band over all *k*-points.

$$P_{iln} = \frac{\sum_{k=1}^{n_k} \sum_{N_i=1}^{n_i} P_{N_i lnk}}{n_k \sum_{k=1}^{n_k} \sum_{N=1}^{n_N} P_{Nlnk}} \times 100\% \qquad (7)$$

where i, N_i, n_i, and N are the ion type, each ion in the ion type, total number of ion in the ion type, and all ions in the unit cell, respectively. The n is the band indices and n_k means the sampled k-points. The P_{iln} is the percentage of

(47) Condron, C. L.; Martin, J.; Nolas, G. S.; Piccoli, P. M. B.; Schultz, A. J.; Kauzlarich, S. M. *Inorg. Chem.* **2006**, *45*, 9381–9386.
(48) Condron, C. L.; Kauzlarich, S. M.; Gascoin, F.; Snyder, G. J. *Chem. Mater.* **2006**, *18*, 4939–4945.
(49) Jung, W.; Loerincz, J.; Ramlau, R.; Borrmann, H.; Prots, Y.; Haarniann, F.; Schnelle, W.; Burkhardt, U.; Baitinger, M.; Grin, Y. *Angew. Chem., Int. Ed.* **2007**, *46*, 6725–6728.

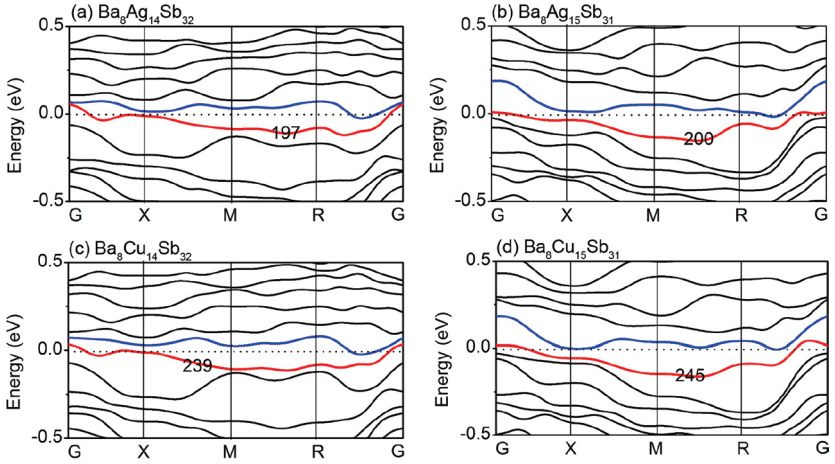

Figure 3. Band structures of selected hypothetical class-I compounds. The valence band edge is marked with band number. G = (0, 0, 0), X = ($^1/_2$, 0, 0), M = ($^1/_2$, $^1/_2$, 0), R = ($^1/_2$, $^1/_2$, $^1/_2$). The Fermi level is set at 0 eV.

the projected wave functional for each ion type with different *l*-quantum in a selected band. The band character decomposition results reveal that Ba 5d for $Ba_8Ga_{16}Ge_{30}$ are 4 and 26% of the eigenstates at the valence band edge (VBE) and the conduction band edge (CBE), respectively, while in both two Sb-based counterparts, $Ba_8Cu_{15}Sb_{31}$ and $Ba_8Ag_{15}Sb_{31}$, Ba 5d states contribute 9.2 and 11% to VBE and CBE, respectively. The Ba 5d states in $Ba_8Ga_{16}Ge_{30}$ contribute inconsiderably at VBE but significantly at CBE, indicating that 5d states are unoccupied and should not influence the VB greatly. By contrary, Ba 5d states in Cu−Sb and Ag−Sb clathrates contribute largely at VBE but indistinguishably at CBE, which may be due to that the Ag 4d or Cu 3d states take 13 or 18% of the eigenstates at VBE, respectively. Therefore, the d states (including Ba 5d, Ag 4d, or Cu 3d) are the important band structure components in class-I compounds. On the other hand, Ba 6s in $Ba_8Ga_{16}Ge_{30}$ is about zero (0.07%) at VBE indicating an almost complete 6s electron-transfer to the framework, which is consistent with the experimental observation by the X-ray absorption near-edge structure (XANES).[50] Differently, Ba 6s states in $Ba_8Ag_{15}Sb_{31}$ contribute 1.4 and 1.6% to VBE and CBE, respectively, indicating an incomplete 6s-electron-transfer to the framework. One possibility is that the valence orbitals of Ba have been overlapped with the frame atom-orbitals; thus, the valence electrons involved in such an overlapping are "shared" rather than "donated" with the frame atoms. The concepts of "share" and "donate" do not mean the conventional covalent bond or ionic bond because the distance between the guest atom and frame atoms is around 4 Å, which is beyond the usual direct bond distance. We have also designed a hypothetical binary model of [$Ag_{15}Sb_{31}$ + 16 e]. The band structure in Figure 4 clearly shows that the bands at both VBE and CBE are dramatically altered, especially at k = $^1/_2$, $^1/_2$, 0. This alteration confirms that Ba is not only an electron donor but also an important participator in the band structures of Cu−Sb- and Ag−Sb clathrates.

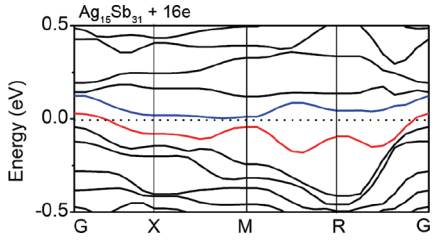

Figure 4. Band structure of model [$Ag_{15}Sb_{31}$ + 16 e].

The VBEs for electron-rich class-I compounds (e.g., band 200 for $Ba_8Ag_{15}Sb_{31}$ and band 245 for $Ba_8Cu_{15}Sb_{31}$) are not filled completely. The structural stability and electronic structures of the corresponding neutral systems have also been studied preliminarily. However, the neutral $Ba_7Ag_{15}Sb_{31}$ is still metallic and is less stable by 42.6 meV/atom than $Ba_8Cu_{15}Sb_{31}$ (Figure S1 in the Supporting Information).

In principle, the band energy for band n with **k**-vector $E(n,\mathbf{k})$ depends on the composition of the *lm*-quantum of each ion in the unit cell. Moreover, this *lm* composition is of course related to the structure characteristics. Therefore, at the same **k**-vector, different configurations should have different band energies. In the following section, we will present the band structures of $Cs_8Zn_{18}Sb_{28}$ and $Cs_8Cd_{18}Sb_{28}$ that are indeed sensitive to the configuration.

Most of band structures of class-II are provided in the Supporting Information. In the following section, calculations on $Cs_8Zn_{18}Sb_{28}$ and $Cs_8Cd_{18}Sb_{28}$, the only two known compounds, will be discussed in detail.

The band structures of three configurations of $Cs_8Zn_{18}Sb_{28}$ and $Cs_8Cd_{18}Sb_{28}$ that have the lowest formation energies, (1, 3, 14), (3, 1, 14), and (3, 6, 9), are plotted in Figure 5. Results show that both compounds of (3, 1, 14) and (3, 6, 9) are metallic, but $Cs_8Zn_{18}Sb_{28}$-(1, 3, 14) is semimetallic and $Cs_8Cd_{18}Sb_{28}$-(1, 3, 14) is metallic. In addition, the density of states (DOS) of $Cs_8Cd_{18}Sb_{28}$ at the Fermi level (E_F) is always slightly higher than that of $Cs_8Zn_{18}Sb_{28}$, thus, $Cs_8Cd_{18}Sb_{28}$ may exhibit a slightly higher electrical conductivity. Contrary to class-I Ag−Sb- or Cu−Sb-clathrates listed in Table 2, Cs 5d and Zn 3d or Cd 4d in class-II compounds are less than 3.5% at band-214 (VBE) and

(50) Bentien, A.; Palmqvist, A. E. C.; Bryan, J. D.; Latturner, S.; Stucky, G. D.; Furenlid, L.; Iversen, B. B. *Angew. Chem., Int. Ed.* **2000**, *39*, 3613–3616.

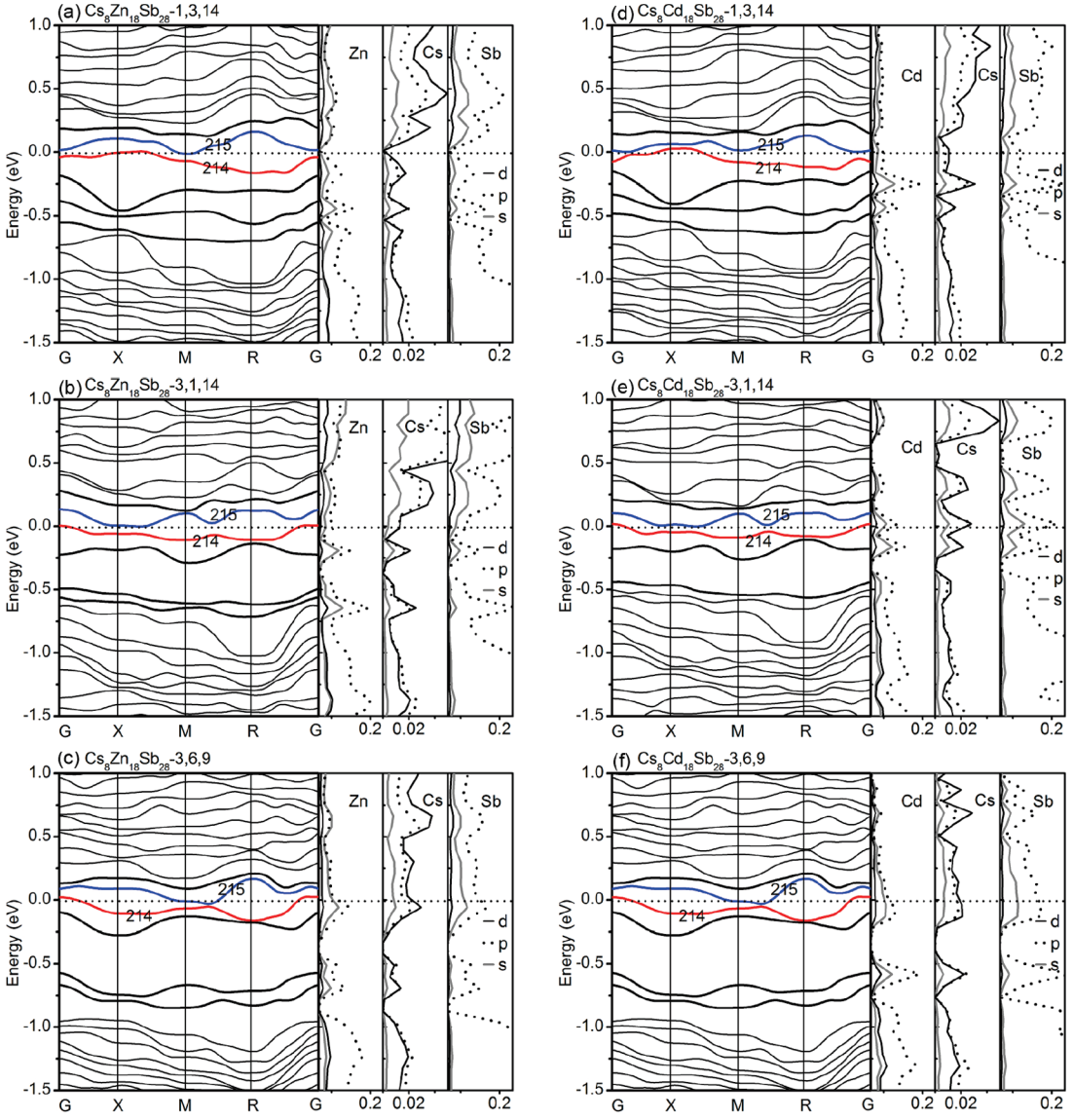

Figure 5. Band structures and density of states of the selected configurations for (a−c) $Cs_8Zn_{18}Sb_{28}$ and (d−f) $Cs_8Cd_{18}Sb_{28}$.

band-215 (CBE) in all the calculated configurations. Unfortunately, the bands of class-II compounds are flat around E_F compared to those of $Ba_8Ga_{16}Ge_{30}$ (Figure S2 in the Supporting Information). According to eq 4, flat bands around E_F should have low electron velocity; according to eqs 2 and 3, flat bands have little contribution to the electrical conductivity. Therefore, the metallic class-II compounds will not exhibit large electrical conductivities.

The band structures of $Cs_8Zn_{16}Sb_{30}$-(3, 1, 12) (Figure S1-8 in the Supporting Information) and $Cs_8Zn_{18}Sb_{28}$-(3, 6, 9) (Figure 5c) clearly show that these compounds are metallic, but in the corresponding regions from −0.5 to −1 eV, several bands below the E_F, both of them have an energy spacing. If E_F could be shifted down by approximately 3 bands 6 electrons for $Cs_8Zn_{16}Sb_{30}$-(3, 1, 12) and 2 bands 4 electrons for $Cs_8Zn_{18}Sb_{28}$-(3, 6, 9), respectively, the thus-generated compounds would have a band gap (E_g). Consequently, two models have been designed, neutral $Cs_2Zn_{16}Sb_{30}$-(3, 1, 12) and electron-poor $Cs_4Zn_{18}Sb_{28}$-(3, 6, 9). The calculations indicate that the composition changes of both models do not noticeably change the overall band shapes with respect to the parent compounds. Model $Cs_2Zn_{16}Sb_{30}$-(3, 1, 12) displays an E_g of about 0.5 eV (Figure 6a) but has a higher formation energy of −24.0 meV/atom than its parent compound $Cs_8Zn_{16}Sb_{30}$-(3, 1, 12) (−162.8 meV/atom, see Table 3). Model $Cs_4Zn_{18}Sb_{28}$-(3, 6, 9) also opens an E_g of 0.3 eV (Figure 6b) but has a comparable formation energy of −192.9 meV/atom to its parent $Cs_8Zn_{18}Sb_{28}$-(3, 6, 9) with −196.7 meV/atom. In addition, as vacancy has been found in type-I clathrate quite often,[7] a vacancy model, $Cs_7Zn_{18}Sb_{25}\square_3$-(3, 6, 9) with three Sb vacancies at 24*k* sites, has also been attempted. Model $Cs_7Zn_{18}Sb_{25}\square_3$-(3, 6, 9) has a very small E_g of 0.03 eV and is quite stable with a formation energy of −217.6 meV/atom. The band shape of $Cs_7Zn_{18}Sb_{25}\square_3$-(3, 6, 9) is totally different from those of $Cs_4Zn_{18}Sb_{28}$-(3, 6, 9) (Figure 6c) and parent $Cs_8Zn_{18}Sb_{28}$-(3, 6, 9) (Figure 5c). Such a narrow E_g may be due to the dangling bond states (DBS)[7] localizing between the valence band and the conduction band. These three

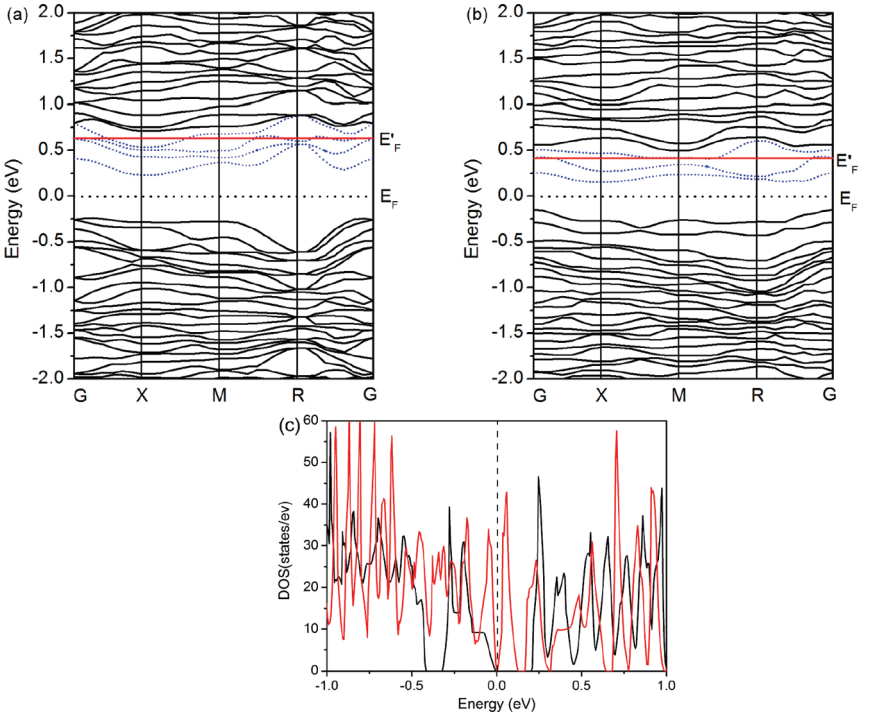

Figure 6. Band structures of (a) neutral $Cs_2Zn_{16}Sb_{30}$-(3, 1, 12), (b) electron-poor $Cs_4Zn_{18}Sb_{28}$-(3, 6, 9). (c) DOS of (black) $Cs_4Zn_{18}Sb_{28}$-(3, 6, 9) and (red) $Cs_7Zn_{18}Sb_{25}\square_3$. E_F is the Fermi level of the models and E_F' is the Fermi level of the parent compounds. The blue dotted lines represent bands from (a) band-205 to band-208 of the parent $Cs_8Zn_{16}Sb_{30}$-(3, 1, 12) and (b) band-213 to band-215 of the parent $Cs_8Zn_{18}Sb_{28}$-(3, 6, 9).

models suggest that it may be possible for a group 12−Sb clathrate to realize a narrow band gap and consequently to be modified as a semiconductor.

At last, we have calculated the transport properties of $Cs_8Zn_{18}Sb_{28}$-(1, 3, 14), $Cs_8Cd_{18}Sb_{28}$-(1, 3, 14), and $Cs_4Zn_{18}Sb_{28}$-(3, 6, 9).

In order to check the reliability of our calculations, we have first calculated the transport properties of the well-established $Ba_8Ga_{16}Ge_{30}$. At room temperature, the Seebeck coefficient (S) for $Ba_8Ga_{16}Ge_{30}$ is measured to be about 79 μV/K with a hole concentration of 3.2×10^{19}.[17] We have obtained a S of 71.3 μV/K with the same hole concentration, which is consistent with the experimental value. Note that if the doping level is high, the calculated S may be wrong. For example, if the electron concentration is -9.3×10^{20}, the calculated and experimental S values are totally different, −26.5 vs −130 μV/K.[17] Therefore, eq 1 may be unsuitable to calculate the heavily doped compounds because of the limitation of the rigid band approach (RBA).[31,32]

The calculated S for $Cs_8Zn_{18}Sb_{28}$ and $Cs_8Cd_{18}Sb_{28}$ are small, −15 and −27 μV/K, respectively. According to eq 1, when $\varepsilon - \mu > 0$, electron as the domain carrier, S is negative; when $\varepsilon - \mu < 0$, hole as the domain carrier, S is positive. If the conduction bands and valence bands are symmetric around E_F, S should be small. Also, the flat band contributes little to S. Thus, a good thermoelectric material is expected to be dominated by one type of carrier and should have very different and dispersive bands around E_F. Band structures of Cu−Sb-, Ag−Sb-, Zn−Sb-, and Cd−Sb-clathrates invariably show that several bands across E_F and the bands around E_F are flat and symmetric (Figure S1 in the Supporting Information); therefore, these compounds are not expected to have large S and electrical conductivities (σ). The maximum power factor ($S^2\sigma$) (around the Fermi level) for p-type or n-type $Ba_8Ga_{16}Ge_{30}$ are about 15 or 9 times higher than those of the corresponding $Cs_8Zn_{18}Sb_{28}$ and $Cs_8Cd_{18}Sb_{28}$, respectively. Note that the terms of n-type and p-type for $Cs_8Zn_{18}Sb_{28}$ and $Cs_8Cd_{18}Sb_{28}$ may be wrong because they are metallic. Those conceptions are used here for the sake of convenience and simple comparison.

The variation of both S and σ to carrier concentration (c) that can be predicted from the Fermi−Dirac distribution:[51]

$$n(\varepsilon_i) = g(i)\frac{1}{e^{(\varepsilon_i - \mu)/\kappa T} + 1} \quad (8)$$

where $g(i)$ and κ are the number of states at energy ε_i and the Boltzmann constant, respectively. Then c is estimated by dividing the number of carriers $n(\varepsilon_i)$ by the unit cell volume. The S vs c at room temperature for $Cs_8Zn_{18}Sb_{28}$ and $Cs_8Cd_{18}Sb_{28}$ are plotted in Figure 7a,b. The electron concentration at E_F is about 6.8×10^{18} cm^{-3} for $Cs_8Zn_{18}Sb_{28}$ and 2.2×10^{19} cm^{-3} for $Cs_8Cd_{18}Sb_{28}$, which indicates again that $Cs_8Cd_{18}Sb_{28}$ is more metallic than $Cs_8Zn_{18}Sb_{28}$. The optimum c (hole or electron) of $Cs_8Zn_{18}Sb_{28}$ is around 3.0×10^{19} cm^{-3}, which is close to the carrier concentration at E_F; a real $Cs_8Zn_{18}Sb_{28}$ compound may easily reach such a concentration level at room temperature, thus, the doping range may be small or the enhancement of the power factor via doping is limited.

Figure 8 plots S and ZT as a function of temperature of $Cs_4Zn_{18}Sb_{28}$-(3, 6, 9) with different carrier concentrations

(51) Leighton, R. B. *Principles of Modern Physics*; McGraw-Hill Education: New York, 1959.
(52) Shimizu, H.; Imai, T.; Kume, T.; Sasaki, S.; Kaltzoglou, A.; Fässler, T. F. *Chem. Phys. Lett.* **2008**, *464*, 54–57.

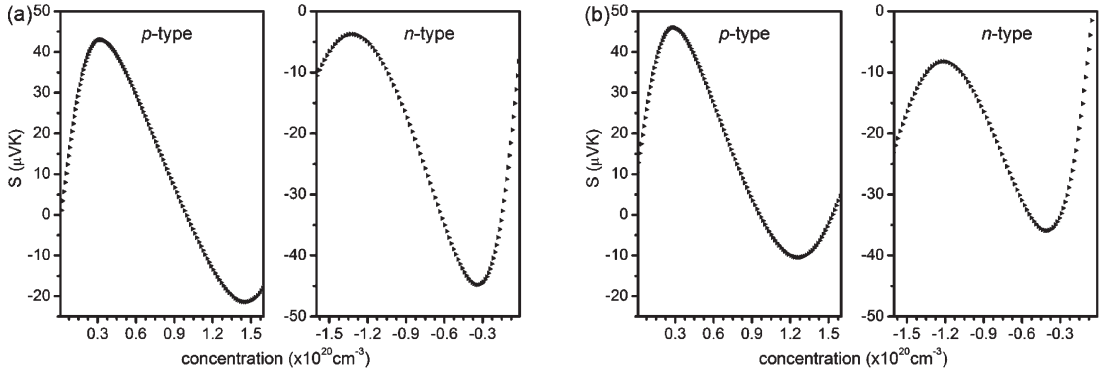

Figure 7. Seebeck coefficient vs carrier concentration at room temperature for (a) $Cs_8Zn_{18}Sb_{28}$-(1, 3, 14) and (b) $Cs_8Cd_{18}Sb_{28}$-(1, 3, 14).

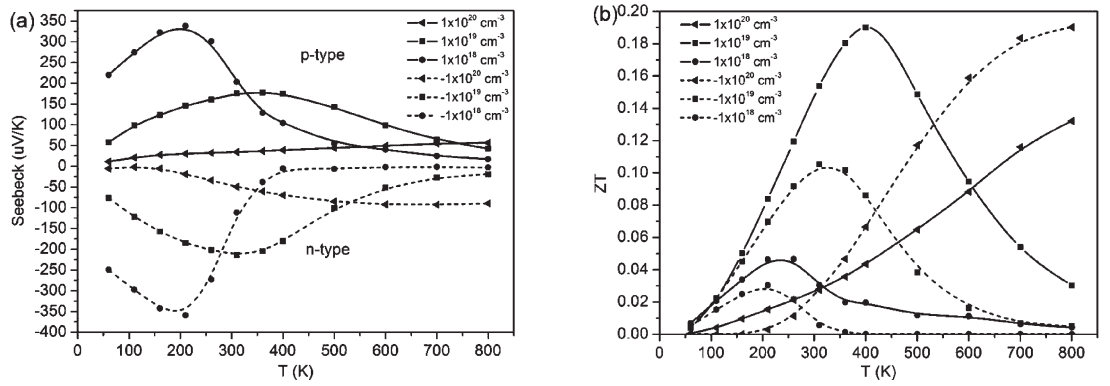

Figure 8. The temperature dependence of the Seebeck coefficient and ZT (assuming $\kappa = 1$ W/mK) of $Cs_4Zn_{18}Sb_{28}$. Solid line, p-type; dashed line, n-type.

under the assumption of thermal conductivity (κ) = 1 W/mK. Figure 8 shows that peak values of S and ZT are realized at around 200 K with low carrier concentration (1×10^{18} cm^{-3}) at 300−400 K with a moderate concentration of 10^{19} cm^{-3}. However, with a higher carrier concentration of 10^{20} cm^{-3}, S and ZT roughly monotonically increase with the temperature increase. Such a carrier concentration related ZT change is of great interest. However, such a concentration-ZT change can be questioned because the assumption of the temperature-independent thermal conductivity might be wrong and GGA is known to underestimate the band gap.

Briefly, the band structure of a Pn-based clathrate is different from that of the Tt-based clathrate by the following points: (1) the guest atom Ba has a great effect on the electronic structure of Sb-based clathrate but not on a Tt-based clathrate. (2) The bands around E_F of $Ba_8Ga_{16}Ge_{30}$ are dispersive and asymmetric, whereas those for $Cs_8Zn_{16}Sb_{30}$ are flat and symmetric. The calculated maximum power factor ($S^2\sigma$) (around E_F) for p-type or n-type $Ba_8Ga_{16}Ge_{30}$ are about 15 or 9 times higher than those of the corresponding $Cs_8Zn_{18}Sb_{28}$ and $Cs_8Cd_{18}Sb_{28}$, respectively.

Conclusions

In this paper, we have studied the structural characteristics and thermoelectric properties of a new family of Sb-based type-I clathrates. The hypothetical structures included all the possible Cu−Sb, Ag−Sb, Zn−Sb, and Cd−Sb frameworks, and the well-known $Ba_8Ga_{16}Ge_{30}$ is studied as a reference. Our LDA calculations on the cell parameters of $Cs_8Zn_{18}Sb_{28}$, $Cs_8Cd_{18}Sb_{28}$, and $Ba_8Ga_{16}Ge_{30}$ are consistent with the experimental data.

The sitting of group 12 elements on the frame sites of $Cs_8Zn_{18}Sb_{28}$ and $Cs_8Cd_{18}Sb_{28}$ clathrates is influenced by radius and coordination geometry. The site preference of Zn or Cd on the Pn-based frame sites is different from that of Ga on a Tt-based framework. The band structures suggest that (1) the guest atom Ba has a great effect on the electronic structure of Sb-based framework but not on that of a Ge-based framework. (2) The bands of $Cs_8Zn_{18}Sb_{28}$ and $Cs_8Cd_{18}Sb_{28}$ are flat and symmetric around E_F. The thermoelectric properties of them are poorer than that of $Ba_8Ga_{16}Ge_{30}$.

Some issues should be explored in the future: (1) The guest−framework interaction is not clear in the Sb-based clathrate. (2) Most of the group 11−Sb- and group 12−Sb-clathrates proposed are metallic, and the corresponding neutral compounds or the compounds with Pn-vacancy are to be studied. Models of neutral $Cs_2Zn_{16}Sb_{30}$-(3, 1, 12), electron-poor $Cs_4Zn_{18}Sb_{28}$-(3, 6, 9), and vacancy derivative $Cs_7Zn_{18}Sb_{25}\square_3$ suggest that the group 12-Sb-based clathrate may have a potential to be modified as a narrow-band gap semiconductor. The effective and reasonable strategies may be interesting.

Acknowledgment. This research was supported by the National Basic Research Program of China (973 Program) Grant 2009CB939801, National Natural Science Foundation

of China under Projects 90922021, 20973175, 20773130, 20733003, and 20821061, the "Knowledge Innovation Program of the Chinese Academy of Sciences" (Grant KJCX2-YW-H20), and the "Key Project from CAS" (Grant KJCX2-YW-H01).

Supporting Information Available: Band structures of class-I and class-II Sb-based type-I clathrates, band structure of $Ba_8Ga_{16}Ge_{30}$, and $M_{site}-M_{site}$ (M = Cd or Zn) bonds of each site configuration (PDF). This material is available free of charge via the Internet at http://pubs.acs.org.